SUPPLEMENTARY FIGURES

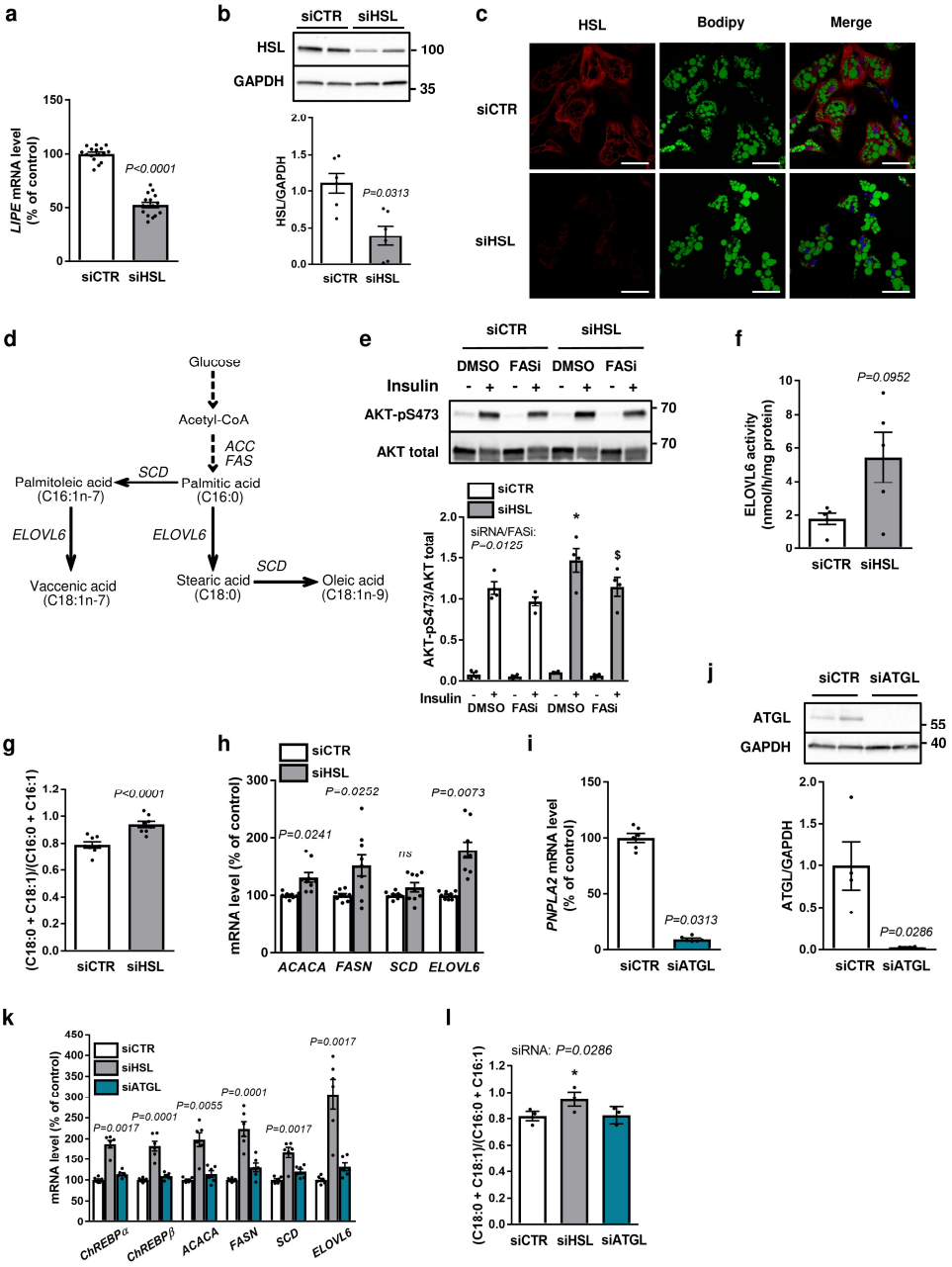

Supplementary Figure 1. (**a, b**) Levels of HSL mRNA (n=16 biologically independent samples per group) (**a**) and protein (n=6 biologically independent samples per group) (**b**) in control (white bars, siCTR) and HSL-deprived (grey bars, siHSL) hMADS adipocytes. GAPDH was used as Western blot loading control. (**c**) Immunodetection of HSL (red) and staining of lipid droplets (Bodipy, green) in control (siCTR) and HSL-deprived (siHSL) hMADS adipocytes. Nuclei were labelled in blue using DAPI (4 independent experiments). Scale bars, 20µm. (**d**) Schematic illustration of the synthesis of fatty acids from glucose in human adipocytes. The main enzymes (in italic) involved are ACC (acetyl CoenzymeA carboxylase); FAS (fatty acid synthase); SCD (stearoyl Coenzyme A desaturase) and ELOVL6 (elongase of very long chain fatty acids protein 6). (**e**) Activating phosphorylation of AKT (pS473) in control (white bars, siCTR) and HSL-deprived (grey bars, siHSL) hMADS adipocytes treated with vehicle (DMSO) or 1µM of fatty acid synthase inhibitor (FASi) for 48h (n=4 biologically

independent samples per group) (Insulin stimulation: P<0.0001). Cropped images of siCTR and siHSL lanes originate from the same blot. DMSO-treated adipocyte values are common to **Supplementary Fig. 1e** and to **Fig. 4d** and **f**. Size markers (in kDa) are shown on illustrative Western blot panel. (**f, g**) ELOVL6 enzymatic activity (n=5 biologically independent samples per group) (**f**) and fatty acid ratio (n=8 biologically independent samples per group) (**g**) in control (white bars, siCTR) and HSL-deprived (grey bars, siHSL) hMADS adipocytes. (**h**) mRNA levels of lipogenic enzymes in control (white bars, siCTR) and HSL-deprived (grey bars, siHSL) differentiated human preadipocytes from primary culture (n=9 biologically independent samples per group). (**i, j**) Levels of ATGL mRNA (n=6 biologically independent samples per group) (**i**) and protein (n=4 biologically independent samples per group) (**j**) in control (white bars, siCTR) and ATGL-deprived (blue bars, siATGL) hMADS adipocytes. Cropped images of siCTR and siATGL lanes originate from the same blot. GAPDH was used as Western blot loading control. (**k, l**) mRNA levels of lipogenic enzymes (n=6 biologically independent samples per group) (**k**) and fatty acid ratio (n=3 biologically independent samples per group) (**l**) in control (siCTR, white bars), HSL (siHSL, grey bars) or ATGL-deprived (siATGL, blue bars) hMADS adipocytes. Data are mean ±sem. Statistical analysis was performed using paired Student's t test (**a, g**), Wilcoxon's test (**b, h, i**), two-way ANOVA with Bonferroni's post hoc tests (**e**), Mann and Whitney's test (**f, j**) or Friedman with Dunn's post-hoc tests (**k, l**). Statistical tests were two-sided. *P<0.05 compared to control. $P<0.05 compared to HSL-deprived adipocytes.

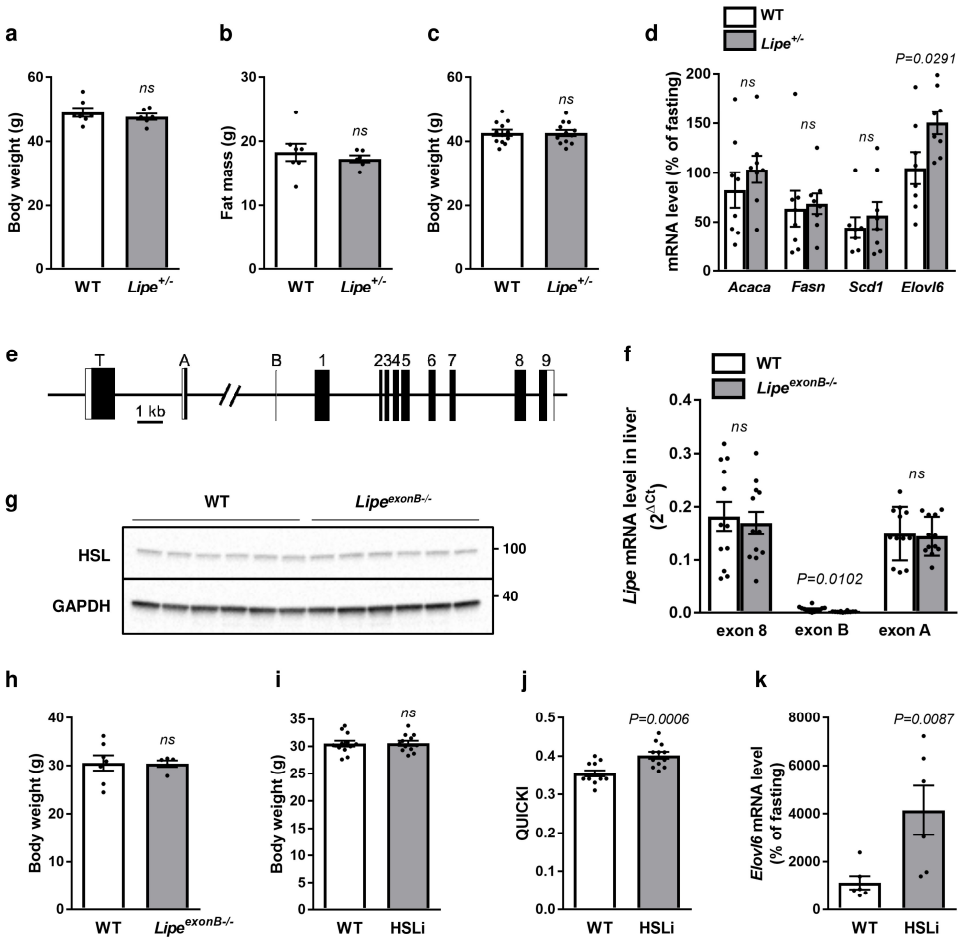

Supplementary Figure 2. (a-d) Experiments were carried out in wild type (WT, white bars) and HSL haploinsufficient (*Lipe*$^{+/-}$, grey bars) mice. (**a, b**) Body weight (**a**) and fat mass (**b**) of B6D2/F1 mice fed 60% high fat diet for 3 months (WT n=7 animals, *Lipe*$^{+/-}$, n=6 animals). (**c**) Body weight of B6D2/F1 mice fed 45% high fat diet for 3 months (n=12 animals per group).

(**d**) mRNA levels of lipogenic enzymes in response to refeeding in gonadal adipose tissue of C57BL/6J mice fed 60% high fat diet for 3 months (n=8 animals per group). (**e**) Schematic representation of the *LIPE* gene. The region upstream of exon 1 contains exons that are expressed in a tissue-dependent and mutually exclusive manner. Exon T is specific of testis transcripts. Exon A is used in pancreatic β-cells and intestine. Exon B is found in adipocyte transcripts. Black rectangles represent coding sequences. Exon 6 encodes the catalytic site Serine (**f-h**) Experiments were carried out in wild type (white bars, WT) and in mice with zinc finger nuclease-mediated deletion of *Lipe* exon B which promoter drives HSL expression in fat cells (grey bars, *Lipe*$^{exonB-/-}$). (**f**) mRNA levels of transcripts containing different exons encoding HSL in liver (n=12 animals per group). (**g**) Western blot analysis (60 µg total protein) of HSL protein content in liver (n= 6 animals per group). GAPDH was used as Western blot loading control. Size markers (in kDa) are shown on illustrative Western blot panel. (**h**) Body weight of wild type (n=7 animals) and *Lipe*$^{exonB-/-}$ (n=5 animals) mice. (**i-k**) Experiments were carried out in mice treated with vehicle (WT, white bars) and a selective HSL inhibitor (HSLi, grey bars) for 11 days. (**i**) Body weight (n=12 animals per group). (**j**) QUICKI (n=12 animals per group). (**k**) mRNA level of *Elovl6* in response to refeeding in gonadal adipose tissue (n=6 animals per group). Data are mean ±sem. Statistical analysis was performed using Mann and Whitney's test (**a, b, h**, **k**) and unpaired Student's t test (**c, d, f, i, j**). Statistical tests were two-sided.

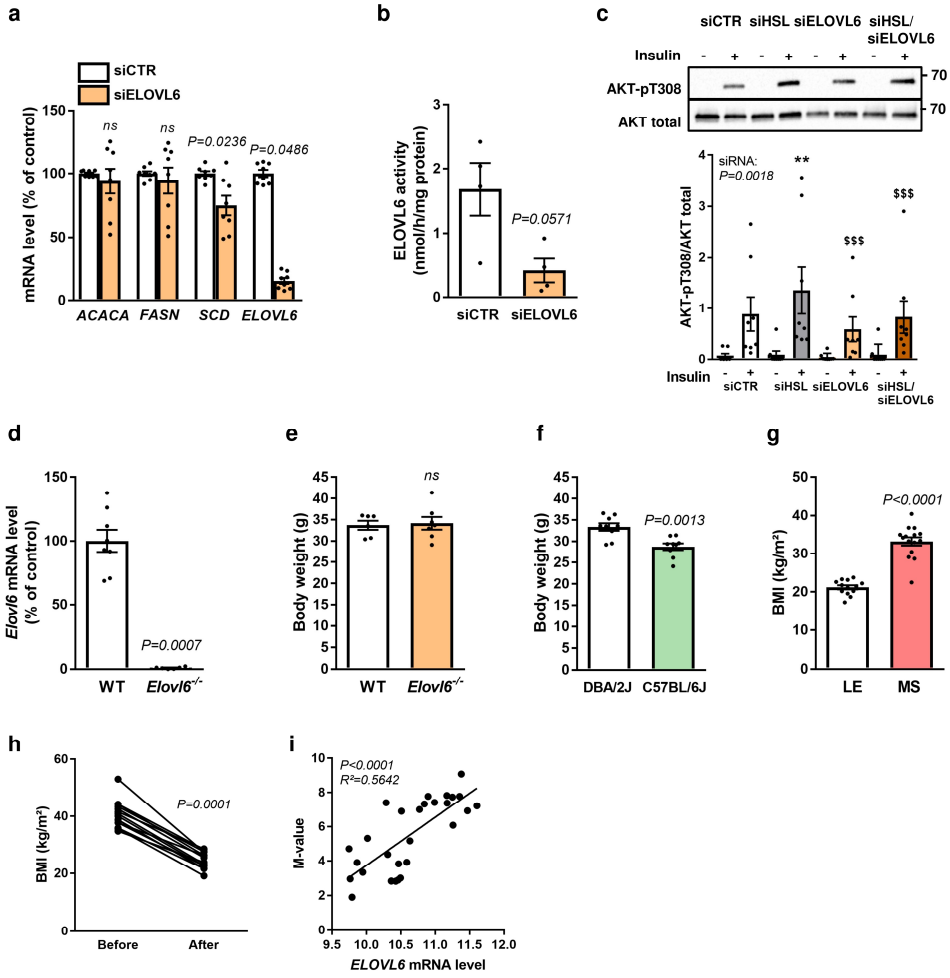

Supplementary Figure 3. (**a, b**) mRNA levels of lipogenic enzymes (n=8 biologically independent samples per group) (**a**) and ELOVL6 enzymatic activity (n=4 biologically independent samples per group) (**b**) in control (white bars, siCTR) and ELOVL6-deprived (light orange bars, siELOVL6) hMADS adipocytes. (**c**) Experiments were carried out in control

(white bars, siCTR), single HSL (grey bars, siHSL), single ELOVL6 (light orange bars, siELOVL6) or dual HSL/ELOVL6-deprived (dark orange bars, siHSL/siELOVL6) hMADS adipocytes in basal (-) and insulin-stimulated (+, 100nM) conditions. Insulin signaling evaluated by activating phosphorylation of AKT (pT308) (n=8 biologically independent samples per group) (Insulin stimulation: P=0.0239). Data from siCTR and siHSL are identical to panel **f** in Fig. 1. Size markers (in kDa) are shown on illustrative Western blot panel. (**d, e**) mRNA level of *Elovl6* in gonadal adipose tissue (**d**) and body weight (**e**) from wild type (WT, white bar, n=8 animals) and *Elovl6* null (*Elovl6*-/-, light orange bar, n=6 animals) mice. (**f**) Body weight of DBA/2J (white bars, n=9 animals) and C57Bl/6J (light green bars, n=9 animals) mice. (**g**) BMI of lean healthy (white bars, LE; n=13 individuals) and obese women with metabolic syndrome (light red bars, MS; n=15 individuals). (**h**) BMI of obese women before and two years after bariatric surgery (n=14 individuals). (**i**) Correlation between adipose *ELOVL6* mRNA level and M-value in obese women (n=28 individuals). Data are mean ±sem. Statistical analysis was performed using paired (**a**) or unpaired Student's t test (**f**), Mann and Whitney's test (**b, d, e, g**), paired two way ANOVA with Bonferroni's post hoc tests (**c**), Wilcoxon's test (**h**), and linear regression (**i**). Statistical tests were two-sided. **P<0.01 compared to control. $^{\$\$\$}$P<0.001 compared to HSL-deprived adipocytes.

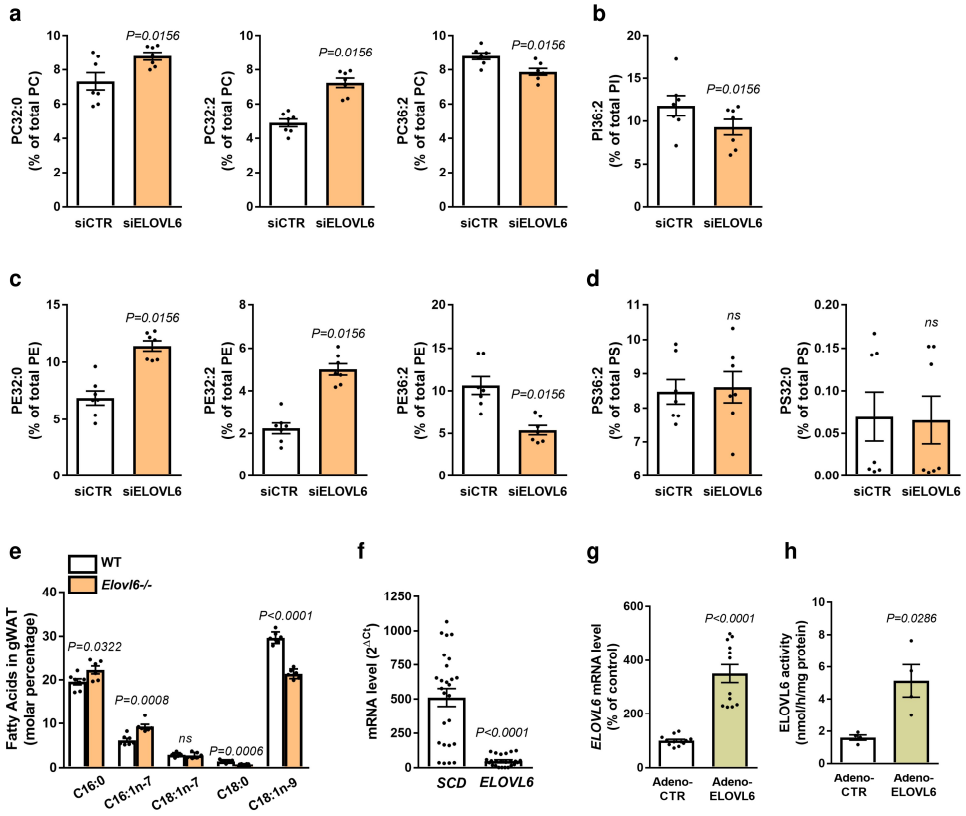

Supplementary Figure 4. (**a-d**) Percentage of PL species with 32:0, 32:2 and 36:2 FAs in total PL (n=7 biologically independent samples per group) in control (white bars, siCTR) and ELOVL6-deprived (light orange bars, siELOVL6) hMADS adipocytes. (**a**) Phosphatidylcholines (PC). (**b**) Phosphatidylinositols (PI). (**c**) Phosphatidylethanolamines (PE). (**d**) Phosphatidylserines (PS). (**e**) Fatty acid composition in gonadal white adipose tissue (gWAT) from wild type (WT, white bars, n=7 animals) and *Elovl6* null (*Elovl6*-/-, light orange bars, n=6 animals) mice. (**f**) *SCD* and *ELOVL6* mRNA levels in hMADS adipocytes (n=26 biologically independent samples per group). (**g-h**) *ELOVL6* mRNA levels (n=12 biologically independent samples per group) (**g**) and enzymatic activity (n=4 biologically independent

samples per group) (**h**) in control hMADS adipocytes expressing GFP (Adeno-CTR, white bar) and in adipocytes expressing human ELOVL6-GFP (Adeno-ELOVL6, avocado bar). Data are mean ±sem. Statistical analysis was performed using Wilcoxon's test (**a-d**), Mann and Whitney's test (**e,h**) and paired Student's t test (**f,g**). Statistical tests were two-sided.

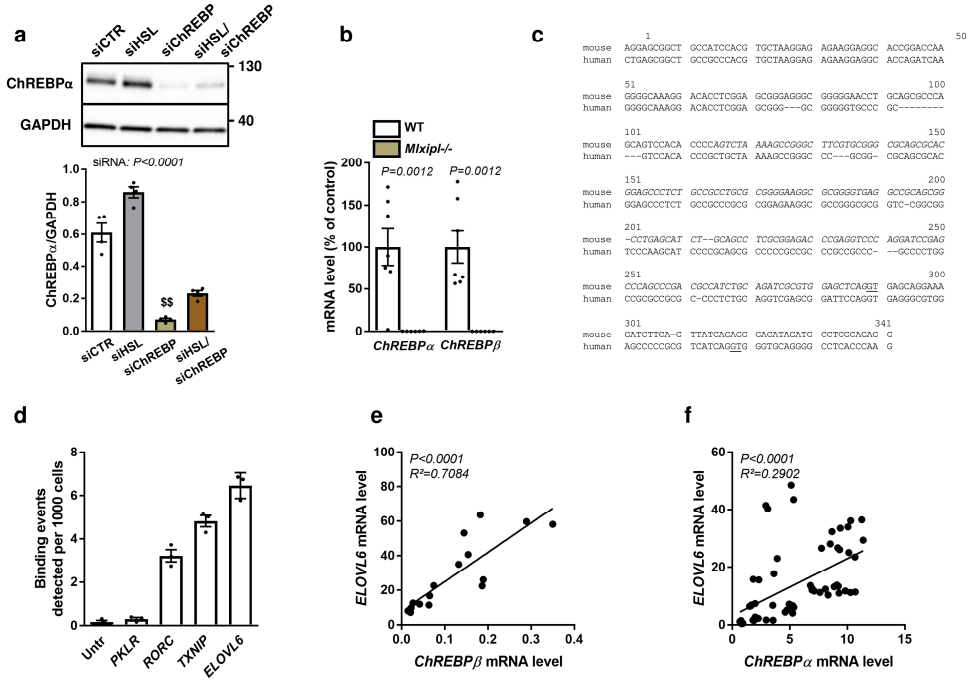

Supplementary Figure 5. (**a**) ChREBPα protein levels in control (white bars, siCTR), single HSL (grey bars, siHSL), single ChREBP (light brown bars, siChREBP) or dual HSL/ChREBP-deprived (dark brown bars, siHSL/siChREBP) hMADS adipocytes (n=4 biologically independent samples per group). Size markers (in kDa) are shown on illustrative Western blot panel. (**b**) mRNA levels of *ChREBPα* and *ChREBPβ* in inguinal adipose tissue of wild type (WT, white bars, n=7 animals) and *ChREBP* null (*Mlxipl*-/-, light brown bars, n=6 animals) mice. (**c**) Murine and human genomic sequences in the ChREBP exon β region. Intron donor sites are underlined. (**d**) Chromatin immunoprepcipitation assays using ChREBP antibody. ChREBP binding on negative (*Untr12*, *PKLR*) and positive control DNA (*RORC*, *TXNIP)* and, on the carbohydrate-responsive element (ChoRE) of *ELOVL6* promoter in hMADS adipocytes. (**e**) Correlation between mRNA levels of *ELOVL6* and *ChREBPβ* in differentiated human preadipocytes from primary culture (n=16 biologically independent samples). (**f**) Correlations between mRNA levels of *ELOVL6* and *ChREBPα* in hMADS adipocytes (n=64 biologically independent samples). Data are mean ±sem. Statistical analysis was performed using Friedman's and Dunn's post hoc tests (**a**), Mann and Whitney's test (**b**) and linear regression (**e, f**). Statistical tests were two-sided. $^{\$\$}$P<0.01 compared to HSL-deprived adipocytes.

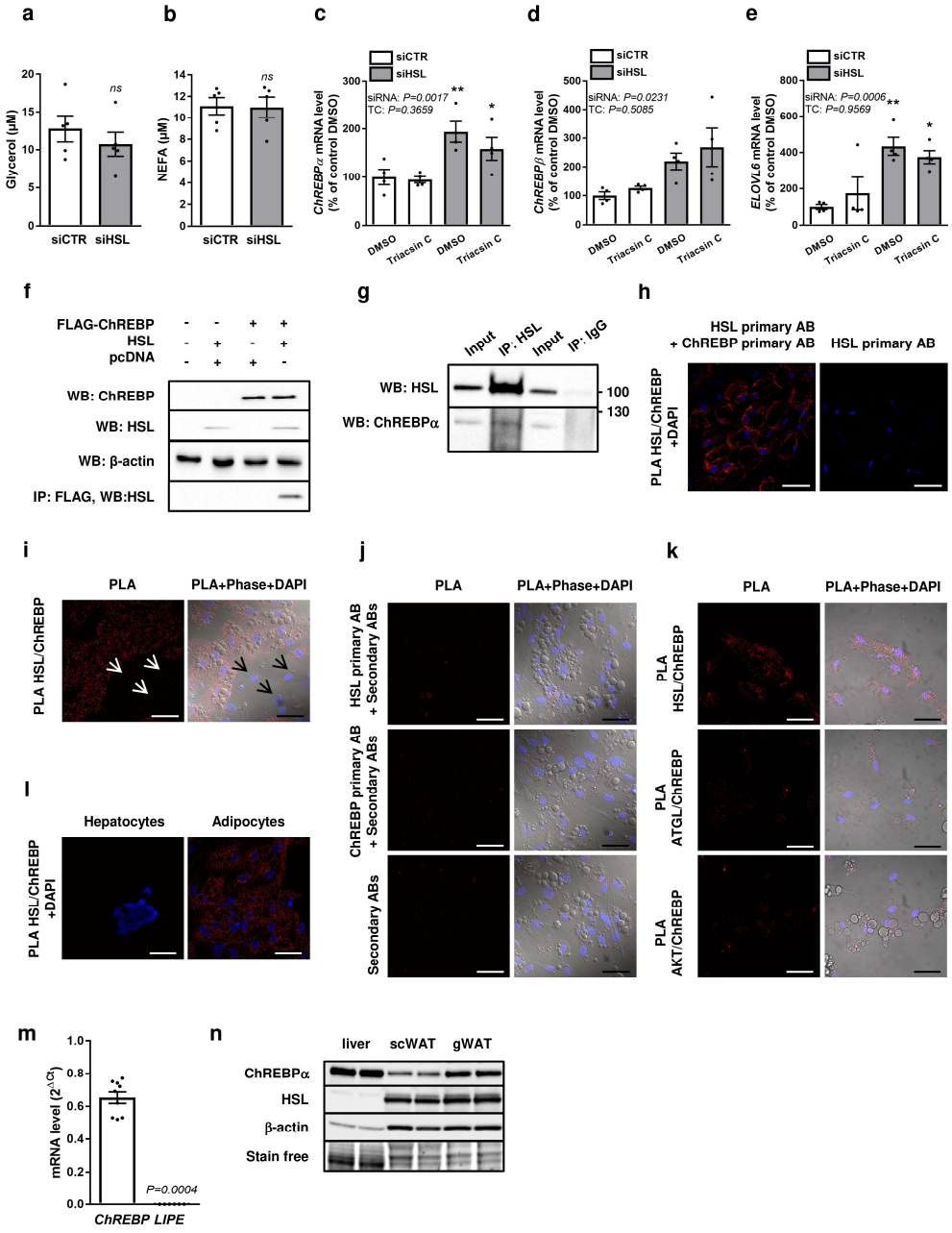

Supplementary Figure 6. (**a-b**) Glycerol (**a**) and non-esterified fatty acid (NEFA) (**b**) levels released in the culture medium for 8h in control (white bars, siCTR) and HSL-deprived (grey bars, siHSL) hMADS adipocytes (n=5 biologically independent samples per group). (**c-e**) mRNA expression levels of *ChREBPα* (**c**), *ChREBPβ* (**d**) and *ELOVL6* (**e**) in control (white bars, siCTR) and HSL-deprived (grey bars, siHSL) hMADS adipocytes treated with vehicle (DMSO) or 10µM of triacsin C for 8h (n=4 biologically independent samples per group). (**f**) Representative image of HSL and ChREBPα immunocomplexes in HEK-293 cells transfected with empty plasmid (pcDNA), FLAG-ChREBP or HSL expression plasmids. β-actin was used as Western blot loading control. Anti-FLAG antibody was used for immunoprecipitation (n=3 independent experiments). (**g**) Endogenous interaction between HSL and ChREBP in human adipocytes. Anti-HSL antibody was used for immunoprecipitation. Normal Mouse IgG antibody was used as negative control (n=2 independent experiments). Size markers (in kDa) are shown on illustrative Western blot panel. (**h**) In situ proximity ligation assays (red signals)

performed with anti-HSL and anti-ChREBP antibodies (PLA HSL/ChREBP) in human adipose tissue (left panel). Negative control was performed using anti-HSL antibody only (right panel). Nuclei were labelled in blue using DAPI. Representative image (n=2 independent experiments). Scale bars, 20µm. (**i**) Representative image of in situ proximity ligation assays in hMADS adipocytes performed with anti-HSL and anti-ChREBP antibodies (PLA HSL/ChREBP, red signals) and corresponding image under visible light (Phase). Nuclei were labelled in blue using DAPI. Arrows indicate undifferentiated fibroblasts. Representative image (n=10 independent experiments). Scale bars, 20µm. (**j**) Negative controls of in situ proximity ligation assays (PLA, red signals) and corresponding image under visible light (Phase) in hMADS adipocytes performed with different combinations of anti-HSL, anti-ChREBP and secondary antibodies (AB). Nuclei were labelled in blue using DAPI. Representative image (n=3 independent experiments). Scale bars, 20µm. (**k**) In situ proximity ligation assays (red signals) performed with different sets of antibodies (anti-HSL/anti-ChREBP, anti-ATGL/anti-ChREBP and anti-AKT/anti-ChREBP) and corresponding image under visible light (Phase) in hMADS adipocytes. Nuclei were labelled in blue using DAPI. Representative image (n=1 independent experiment). Scale bars, 20µm. (**l**) In situ proximity ligation assays (red signals) performed with anti-HSL and anti-ChREBP antibodies (PLA HSL/ChREBP) in human HepG2 hepatocytes and hMADS adipocytes. Nuclei were labelled in blue using DAPI. Representative image (n=1 independent experiment). Scale bars, 20µm. (**m**) *ChREBP* and *LIPE* mRNA levels in HepG2 hepatocytes (n=9 biologically independent samples per group). (**n**) Western blot analysis (30 µg total protein) of ChREBP and HSL protein content in liver, subcutaneous (sc) and gonadal (g) white adipose tissue (WAT). β-actin and stain free were used as Western blot loading control. Data are mean ±sem. Statistical analysis was performed using two-sided Wilcoxon's test (**a, b**), paired two-way ANOVA with Bonferroni's post hoc tests (**c-e**) or Mann and Whitney's test (**m**). Statistical tests were two-sided. *P<0.05, **P<0.01 compared to control adipocytes (c-e).

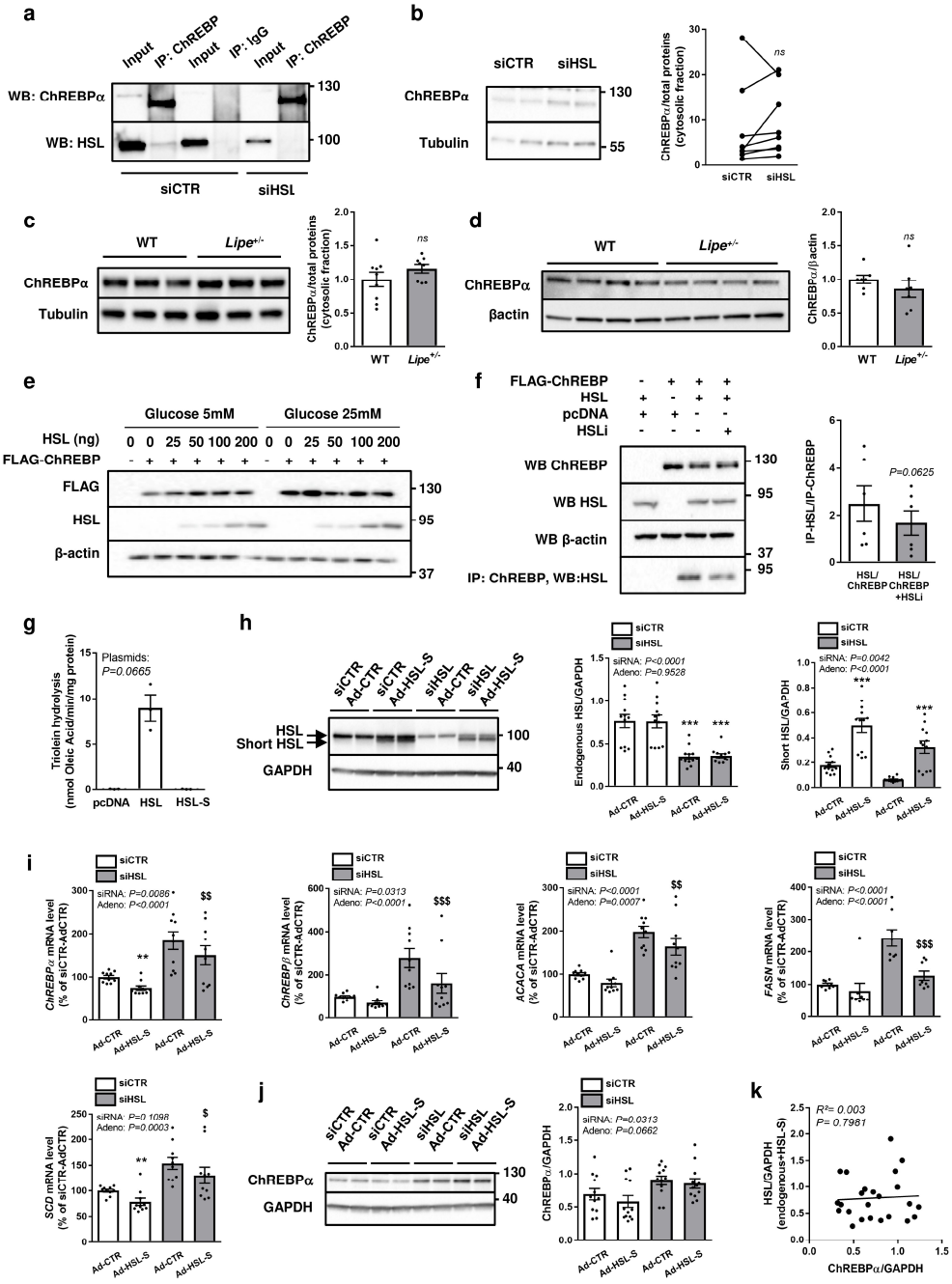

Supplementary Figure 7. (**a**) Representative image of ChREBPα and HSL immunocomplexes in control (siCTR) and HSL-deprived (siHSL) hMADS adipocytes. Anti-ChREBP antibody was used for immunoprecipitation. Normal Rabbit IgG antibody was used as negative control for immunoprecipitation (n= 4 independent experiments). (**b**) ChREBPα protein levels in cytosolic extracts from control (siCTR) and HSL-deprived (siHSL) hMADS adipocytes (n=8 biologically independent samples per group). (**c**) ChREBPα protein levels in cytosolic extracts from white adipose tissue of wild type (WT, n=8 animals) and *Lipe*$^{+/-}$ (n=9 animals) mice. (**d**) ChREBPα protein levels in whole extracts from white adipose tissue of wild type (WT, n=7 animals) and *Lipe*$^{+/-}$ (n=7 animals) mice. β-actin was used as Western blot loading control. (**e**) Protein levels of ChREBP and HSL in HEK-293 cells transfected with pcDNA (-), ChREBP (+) or HSL (indicated ng) expression plasmids (n= 1 independent experiment). (**f**) HSL and ChREBP immunocomplexes in HEK-293 cells transfected with empty plasmid (pcDNA3) or with FLAG-ChREBP and/or HSL expression plasmids and treated with 10μM of a specific

HSL inhibitor (HSLi). β-actin was used as Western blot loading control. Anti-FLAG antibody was used for immunoprecipitation (n=5 biologically independent samples per group). (**g**) Lipase activity of HSL isoforms. Cos-7 cells were tranfected with control (pcDNA), full length HSL (HSL) and HSL short form (HSL-S) expression vectors. In vitro hydrolysis of triolein into oleic acid was measured (n=3 biologically independent experiments). (**h-k**) Effect of overexpression of the short inactive form of HSL (HSL-S) in hMADS adipocytes. Experiments were carried out in control (siCTR, white bars) and HSL-deprived (siHSL, grey bars) hMADS adipocytes overexpressing green fluorescent protein (GFP, Ad-CTR) or the short inactive form of HSL (Ad-HSL-S). (**h**) Protein levels of full length HSL and short form HSL (n=12 biologically independent samples per group). GAPDH was used as Western blot loading control. (**i**) mRNA levels of *ChREBP* isoform and lipogenic enzymes (n=10 biologically independent samples per group). (**j**) Protein levels of ChREBPα (n=12 biologically independent samples per group). GAPDH was used as Western blot loading control. Size markers (in kDa) are shown on illustrative Western blot panels. (**k**) Correlations between protein levels of HSL and ChREBPα (n=24 biologically independent samples). Data are mean ± sem. Statistical analyses was performed using paired Student's t test (**b**), Mann and Whitney's test (**c, d**), Wilcoxon's test (**f**), Kruskal-Wallis with Dunn's post-hoc tests (**g**), two-way ANOVA with Bonferroni's post-hoc tests (**h-j**) and linear regression (**k**). Statistical tests were two-sided. **P<0.01 ***P<0.001 compared to siCTR adipocytes. $^{\$}$P<0.05, $^{\$\$}$P<0.01, $^{\$\$\$}$P<0.001 compared to siHSL adipocytes.

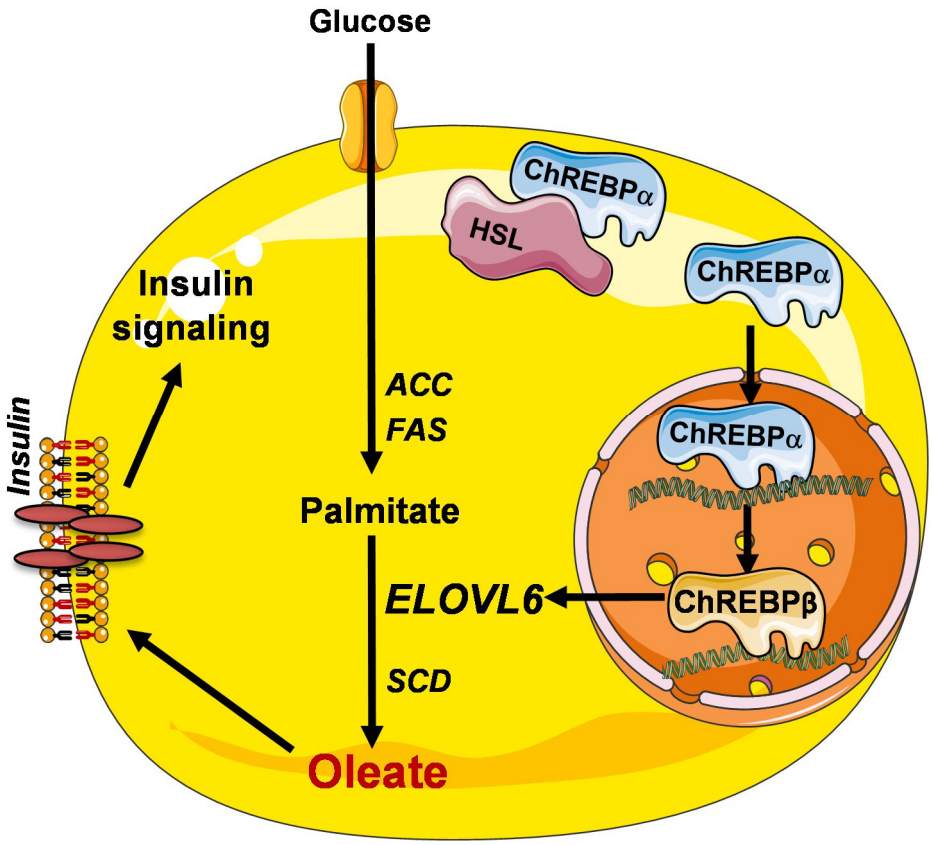

Supplementary Figure 8. Schematic description of the HSL/ChREBP/ELOVL6 pathway controlling fat cell insulin signaling. HSL interacts with ChREBPα and inhibits the transcription factor nuclear translocation. ChREBP, especially the superactive form ChREBPβ, by a positive control of ELOVL6 is responsible of an increase in oleic acid synthesis. Increased phospholipid oleic acid modifies plasma membrane properties and improves insulin signaling.

Figure 1

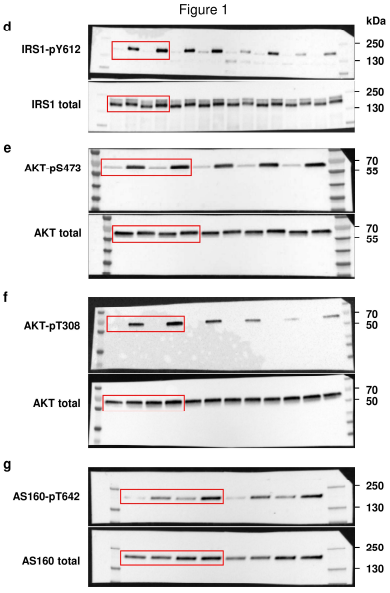

Figure 2

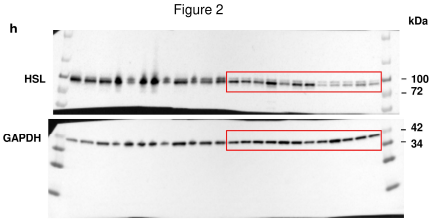

Figure 3

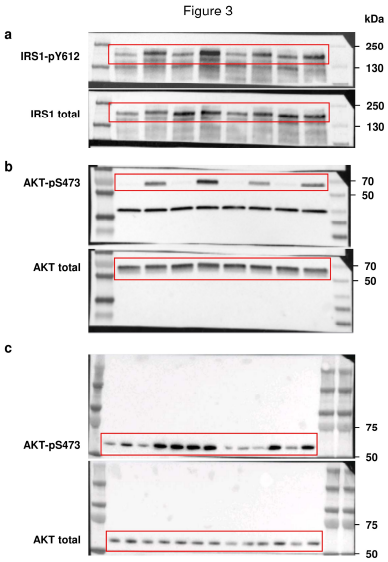

Figure 4

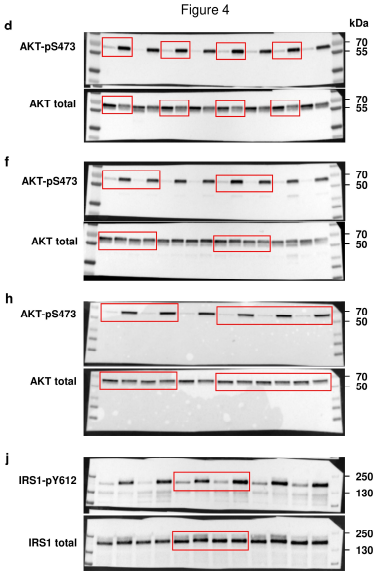

Figure 5

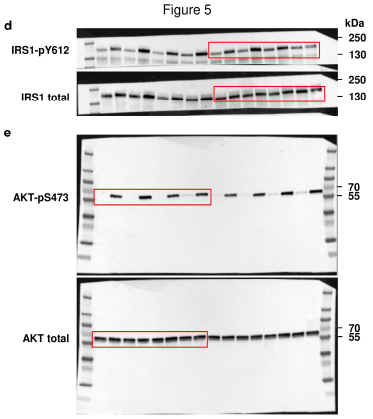

Figure 6

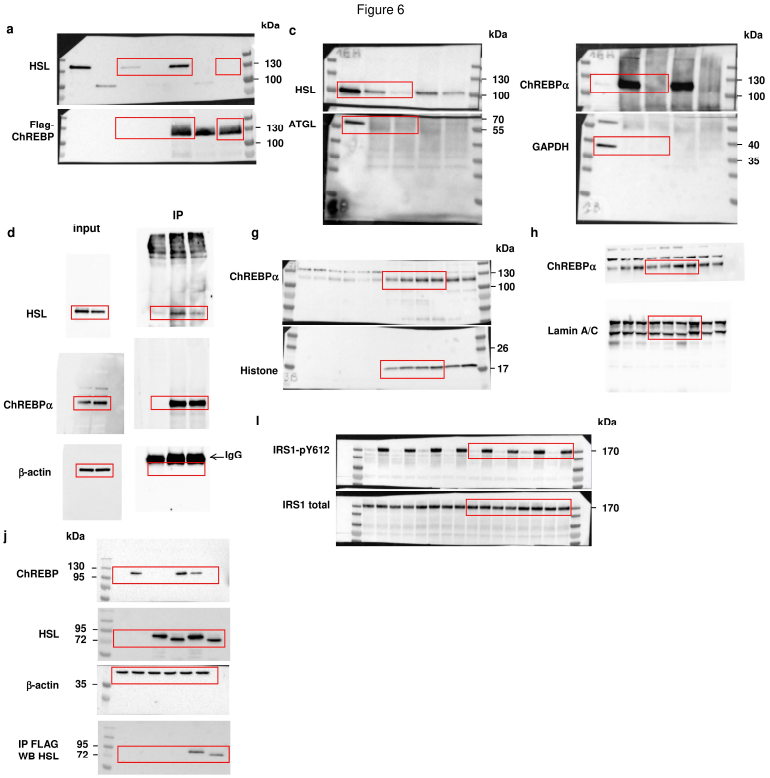

Supplementary Figure 1

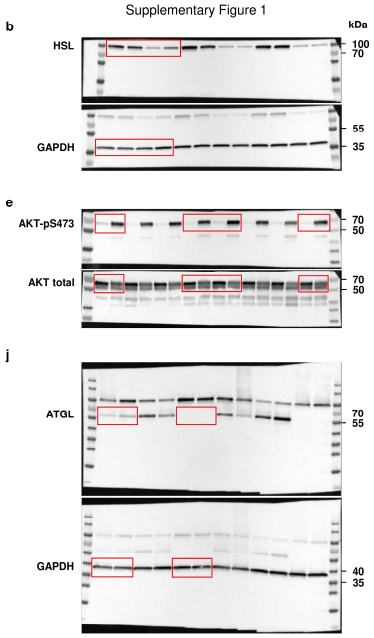

Supplementary Figure 2

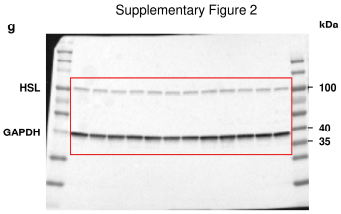

Supplementary Figure 3

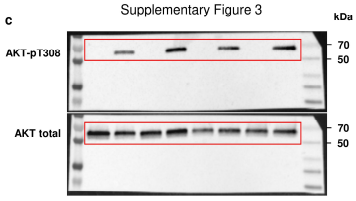

Supplementary Figure 5

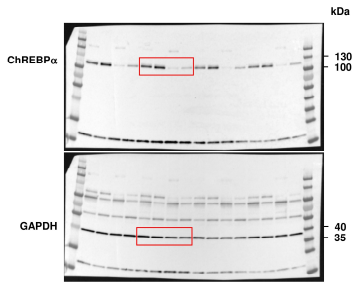

Supplementary Figure 6

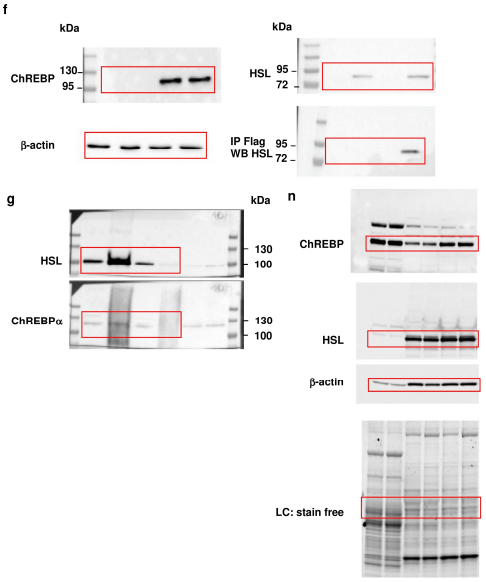

Supplementary Figure 7

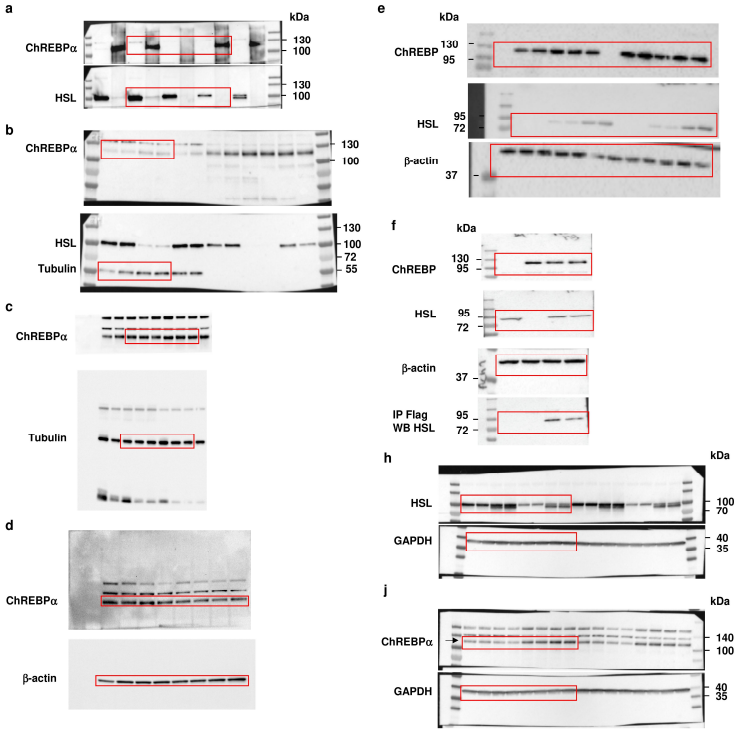

Supplementary Figure 9. Full scans of Western blots. Specific bands shown in the figures are highlighted by red boxes

SUPPLEMENTARY METHODS

Culture of human adipocytes and in vitro measurements.

HEK293 and HepG2 cell cultures. HEK293 cells (ATCC-CRL-3216) were cultured in DMEM supplemented with 10% fetal calf serum (Sigma). HepG2 hepatocytes (ATCC-HB-8065) were cultured in Eagle's Minimum Essential Medium (Life Technologies) with 10% fetal bovine serum.

RNA interference. Targeted sequences, flanked with dTdT overhangs, are: GFP, 5'-GCAGCACGACUUCUUCAAG-3'; HSL, 5'-AGGACAACAUAGCCUUCUU-3'; ChREBP, n°1: 5'ACAAGAAGCGGCUCCGUAA-3', n°2: 5'-GCAAACAGCUCUUCUCCAG-3', n°3: 5'-GACACUCUCUUCACCAUGA-3', n°4: 5'-UCUCUUCUCUCCCAGGUUU-3'; ELOVL6, n°1: 5'-CGAACUAGGAGAUACAAUA-3', n°2: 5'-CAGAAGCAGAGGAGACUAA-3', n°3: 5'-GAGUGGCAAUACUACAACA-3'; ATGL, 5'-AGUUCAUUGAGGUAUCUA A-3'.

Plasmid transfection. HEK293 cells were transfected using lipofectamine 2000 (Invitrogen) with 1µg each of 5' FLAG-tagged ChREBP, HSL expression and empty plasmids [1,2] unless otherwise indicated. HEK293 cells were harvested 48h after transfection.

Oleic acid supplementation in human adipocytes. For oleic acid supplementation experiments, hMADS adipocytes were treated for 48 hours with 100µM and 500µM of oleic acid (O1383-1G, Sigma) previously bound to 0.7% of fatty acid-free bovine serum albumin (Sigma).

Gene expression analysis. Cells were scraped in RLT-β mercaptoethanol 1%. Total RNA was extracted using RNeasy kit (Qiagen). After treatment with DNase I (Invitrogen) and reverse transcription of total RNA with high capacity cDNA reverse transcription kit (Applied Biosystems), real-time quantitative PCR was performed using Applied Biosystems ViiA7 real-time PCR system. *LRP10* [Hs00204094_m1], *LIPE* [Hs00943404-m1], *PNPLA2* [Hs00982040_g1], *ACACA* [Hs00167385_m1], *FASN* [Hs00188012_m1], *SCD* [Hs01682761_m1] and *ELOVL6* [Hs00907564_m1] mRNA levels were determined using Taqman Fast Advanced Master Mix (Applied Biosystems). ChREBPα (*MLXIPL* gene) (forward : AGTGCTTGAGCCTGGCCTAC ; reverse : TTGTTCAGGCGGATCTTGTC), ChREBPβ (*MLXIPL* gene) (forward : AGCGGATTCCAGGTGAGG ; reverse : TTGTTCAGGCGGATCTTGTC) and *ELOVL6* (forward : CCATCCAATGGATGCAGGAAAAC ; reverse : CCAGAGCACTAATGGCTTCCTC) expression were evaluated using Fast SYBR Green Advanced Master Mix. *LRP10* was used as control to normalize gene expression.

Characterization of human ChREBPβ-specific exon. Following reverse transcription of hMADS adipocyte RNA, PCR was performed with different couples of primers PCR1: forward, CAGGTCGAGCGGATTCCAG ; reverse, GCTCTTCCTCCGCTTCACATA; PCR2: forward, CAGGTCGAGCGGATTCCAG ; reverse, TTGTTCAGGCGGATCTTGTC; PCR3: forward, AGCGGATTCCAGGTGAGG ; reverse, GCTCTTCCTCCGCTTCACATA. PCR products were sequenced using BigDye Terminator v3.1 Cycle Sequencing Kit and 3130xl Genetic Analyzer with POP-7 polymer (Thermo Fischer Scientific).

Western blot analysis. For protein analysis, insulin was removed during the day before the assay and cells were stimulated with or without 100nM insulin for 50 min. Primary anti-phospho-tyrosine 612-IRS1 (1/1000, 44816G, Invitrogen), anti-phospho-serine 473-AKT (1/1000, 4060, Cell Signaling Technology, anti-phospho-threonine 308-AKT (1/1000, 2965, Cell Signaling Technology) and anti-phospho-threonine 642-AS160 (1/500, 4288, Cell Signaling Technology) antibodies were used for insulin signaling studies. Total IRS1 (1/1000, 3407, Cell Signaling Technology), total AKT (1/1000, 4691, Cell Signaling Technology) or total AS160 (1/500, 2670, Cell Signaling Technology) antibodies were used for normalization. For lipases and ChREBP protein levels measurements, anti-HSL (1/1000, 4107, Cell Signaling Technology), anti-ATGL (1/1000, 2138, Cell Signaling Technology) and anti-ChREBP (1/1000, NB400-135,

Novus) primary antibodies were used. GAPDH (1/5000, 2118, Cell Signaling Technology) and β–actin (1/1000, 4970, Cell Signaling Technology) were used as loading control.
Fatty acid composition in phospholipid classes. Cells were scraped in PBS and stored at -80°C. Lipids were extracted from adapted Bligh and Dyer. First, samples were supplemented in 5mM EGTA water and methanol (1:2). Internal standards were added (Cer d18:1/15:0 16 ng ; SM d18:1/12:0 16 ng, PE 12:0/12:0 180 ng , PC 13:0/13:0 16 ng , PI 16:0/17:0 30 ng, PS 12:0/12:0 156.25 ng (Avanti Polar Lipids). Phospholipids were extracted in methanol 2% acetic acid, water and chloroform (2.5: 2: 2.5). After centrifugation (1500rpm, 3min), organic phase was isolated and dried under nitrogen. Samples were then re-suspended in 50µL methanol and stored at -20°C before analysis by LC-MS/MS (HPLC system (Agilent 1290 Infinity) coupled on-line to an Agilent 6460 triple quadrupole MS (Agilent Technologies).
Measurement of glycerol and NEFA in culture medium. For lipolysis analyses, cells were exposed to 0.5% BSA (Sigma) solution in the culture medium for 8h. Glycerol and NEFA released in the medium were measured using commercially available kits (free glycerol reagent from Sigma and NEFA-C from Wako chemicals).
Luciferase activity. HEK293 cells were transfected using 50 ng of a luciferase reporter construct containing three copies of the highly conserved L4L3 region of the rat L-PK promoter with a well characterized ChoRE [3]. Co-transfection experiments were performed using 50 ng of ChREBP, 50 ng of Mlx and 50 ng of β-galactosidase plasmids. Increasing amounts of HSL plasmid were as indicated in Fig. 6g. Luciferase assay was performed after cell lysis 24 post-transfection. β-galactosidase assays were performed for normalization of ChoRE-luciferase activity.

Animal studies.
Gene and protein expression analyses. For gene analysis of *Lipe* and *Mlxipl* mouse models, total RNA extraction, reverse transcription and quantitative PCR were the same as described above. *Scd1* [Mm01197142_m1] and *Elovl6* [Mm04209852_g1] mRNA levels were determined using Taqman Fast Advanced Master Mix (Applied Biosystems). *Hprt* (forward, TGGCCATCTGCCTAGTAAAGC; reverse, GGACGCAGCAACTGACATTTC), *Lipe* (forward, ACTCAACAGCCTGGCAAAAT; reverse, AGGTCACAGTGCTTGACAGC), *Lipe* exon A (forward, ATCGAAGAACCGCAGTCGCA; reverse, ATGCTGTGTGAGAACGCTGA), *Lipe* exon B (forward, CAGACCTGCTGTGCCAGC; reverse, ATGCTGTGTGAGAACGCTGA), *Lipe* exon 8 (forward, GGCTTACTGGGCACAGATACCT; reverse, CTGAAGGCTCTGAGTTGCTCAA), *Mlxipl* (forward, CACTCAGGGAATACACGCCTAC; reverse, ATCTTGGTCTTAGGGTCTTCAGG), *Acaca* (forward, GCCTCTTCCTGACAAACGAG; reverse, TGACTGCCGAAACATCTCTG) and *Fasn* (forward, TGGTGAATTGTCTCCGAAAAG; reverse, CACGTTCATCACGAGGTCATG) expression were evaluated using Fast SYBR Green Advanced Master Mix. *Hprt* was used as control to normalize gene expression. Data are expressed in percentage of fasting or in percentage of control condition.
For protein analysis of *Lipe* mouse models, adipose tissue and liver were homogenized in RIPA buffer containing protease and phosphatase inhibitors (Sigma) using Precellys homogenizer and centrifuged. Supernatants were harvested for determination of total protein concentration. Protein analysis was performed as described above.
For gene and protein analyses of *Elovl6* null mice, RNA from the gonadal white adipose tissue of wild type and Elovl6 null mice was extracted using STAT-60 (AMS Biotech). Reverse transcription was performed using Reverse Transcriptase System (Promega). Real-time PCR was carried out using Sybr Green reagents using an ABI 7900 real-time PCR machine using default thermal cycler conditions. Gonadal white adipose tissue from wild-type and *Elovl6* null

mice was homogenized in RIPA buffer containing protease inhibitors (Roche Complete) and phosphatase inhibitors (Roche PhosSTOP phosphatase inhibitor cocktail). SDS page and Western blotting was performed using the NuPAGE system and iBlot (Invitrogen). Membranes were probed using antibodies against pAKT-S473 (4060, Cell Signaling Technology) and total AKT (9272, Cell Signaling Technology).

Measurement of fasting glucose and insulin. For QUICKI calculation (1/[log(I0) + log(G0)], where I0 is fasting insulin (μU/ml) and G0 is fasting glucose (mg/dl)), fasting plasma glucose and insulin were determined respectively with a Glucotrend Accu-Chek Performa (Roche SAS) and by ELISA (Mercodia).

Glucose and insulin tolerance tests and insulin bolus injection. For glucose and insulin tolerance tests, 1 mg/g body weight of D-(+) glucose (Sigma) and 0.6mU/g body weight of insulin (Lilly) were administered by intraperitoneal route to overnight and 6h fasted mice, respectively. Glycemia was checked on blood from tail vein 30 min and 15 min before glucose injection and then at various times after glucose administration with a Glucotrend Accu-Chek Performa (Roche SAS). For insulin bolus experiments, mice were fasted over-night and injected with 2.5U/kg of insulin or PBS control. Mice were culled 10 minutes after insulin injection.

Euglycemic-hyperinsulinemic clamp. A catheter was inserted into the femoral vein on anaesthetized animals by isoflurane. Body weight was monitored during all the postsurgical period. After 3 day of recovery, mice were fasted during 6h. Basal plasma glucose was measured before the beginning of the experiment. At the beginning of the clamp, every mouse received a bolus of insulin (5.4 mU/mice) and was then perfused with insulin (18mU/kg/min). Radiolabelled ^{3}H-glucose was also perfused at the same time (bolus of 30μCi/mice followed by a 30μCi/min/kg perfusion). Euglycemia was maintained at 100mg/dl by adjusting the glucose perfusion. At the end of the clamp, blood sampling was performed at the retro-orbital sinus.

Human research.

Gene expression analysis. For women with differing obese and metabolic status, procedures were similar as for human adipocytes described above. For hyperglycemic hyperinsulinemic clamp in young men, total RNA from abdominal subcutaneous adipose tissue was obtained using RNeasy mini kit (Qiagen). 500ng of total RNA were reverse transcribed using Superscript II (Thermo Fischer Scientific). mRNA levels were evaluated using SYBR qPCR Premix Ex Taq (Tli RNaseH Plus) (Ozyme) with RotorGene 6000 (Qiagen). *TBP* (forward, TGGTGTGCACAGGAGCCAAG; reverse, TTCACATCACAGCTCCCCAC) was used as control to normalize gene expression. Other primer sequences are mentioned above. For morbidly obese subjects undergoing bariatric surgery, subcutaneous fat biopsy specimen was obtained by needle aspiration under local anesthesia from the mid-abdominal area. It was rapidly washed in saline and immediately thereafter frozen at -70ºC. All samples (before/after surgery) were simultaneously extracted for RNA and subsequent micro-array analyses as described in Dahlman *et al.* [4] using the Gene 1.1 ST Arrays (Affymetrix Inc., Santa Clara, CA, USA).

SUPPLEMENTARY REFERENCES

1. Laurell, H.*, et al.* Species-specific alternative splicing generates a catalytically inactive form of human hormone-sensitive lipase. *Biochem J* **328 (Pt 1)**, 137-143 (1997).
2. Stoeckman, A.K., Ma, L. & Towle, H.C. Mlx is the functional heteromeric partner of the carbohydrate response element-binding protein in glucose regulation of lipogenic enzyme genes. *J Biol Chem* **279**, 15662-15669 (2004).

3. Lou, D.Q.*, et al.* Chicken ovalbumin upstream promoter-transcription factor II, a new partner of the glucose response element of the L-type pyruvate kinase gene, acts as an inhibitor of the glucose response. *J Biol Chem* **274**, 28385-28394 (1999).
4. Dahlman, I.*, et al.* The fat cell epigenetic signature in post-obese women is characterized by global hypomethylation and differential DNA methylation of adipogenesis genes. *Int J Obes (Lond)* **39**, 910-919 (2015).